

# Brain organization into resting state networks emerges from the connectome at criticality

Ariel Haimovici,<sup>1,2</sup> Enzo Tagliazucchi,<sup>3</sup> Pablo Balenzuela,<sup>1,2</sup> and Dante R. Chialvo<sup>2,4,5</sup>

<sup>1</sup>*Departamento de Física, Facultad de Ciencias Exactas y Naturales,  
Universidad de Buenos Aires, Buenos Aires, Argentina*

<sup>2</sup>*Consejo Nacional de Investigaciones Científicas y Tecnológicas, Buenos Aires, Argentina.*

<sup>3</sup>*Neurology Department and Brain Imaging Center,  
Goethe University, Frankfurt am Main, Germany.*

<sup>4</sup>*Facultad de Ciencias Médicas, Universidad Nacional de Rosario, Rosario, Argentina*

<sup>5</sup>*David Geffen School of Medicine, University of California Los Angeles, Los Angeles, CA, USA*  
(Dated: September 25, 2012)

The relation between large-scale brain structure and function is an outstanding open problem in neuroscience. We approach this problem by studying the dynamical regime under which realistic spatio-temporal patterns of brain activity emerge from the empirically derived network of human brain neuroanatomical connections. The results show that critical dynamics unfolding on the structural connectivity of the human brain allow the recovery of many key experimental findings obtained with functional Magnetic Resonance Imaging (fMRI), such as divergence of the correlation length, anomalous scaling of correlation fluctuations, and the emergence of large-scale resting state networks.

Understanding the relation between brain architecture and the behavioral repertoire it produces is a central question in neuroscience. In that direction, important efforts over recent years have been devoted to map the large-scale structure of the human cortex, including attempts to build brain structural connectivity matrices from imaging data. An example is the connectivity matrix of the entire human brain, recently derived from fiber densities measured between a large number (500-4000) of homogeneously distributed brain regions [1]. This and related work encompasses a large collaborative project dubbed the brain “connectome” [2], whose ultimate goal is to understand in detail the architecture of whole-brain connectivity. The question discussed in this Letter is how much of the experimentally observed brain dynamics can be then expounded from such detailed knowledge of brain connectivity. In other words, and using a simple analogy: how much of the large-scale traffic dynamics of a city can be predicted from a very detailed map of all streets?. The results presented in this Letter show that very relevant aspects of brain dynamics can be predicted from the structure providing that the underlying dynamics are critical.

To guide our comparison with available experimental results, we choose to concentrate on robust findings concerning brain dynamics. Specifically, we wish to ask how spontaneous brain dynamics at the large scale organize into the relatively few spatio-temporal patterns revealed experimentally in recent years [3]. This is important because a wide range of experiments using functional Magnetic Resonance Imaging (fMRI) have repeatedly emphasized that these spatial clusters of coherent activity, termed Resting State Networks (RSN) [4], are associated with specific sensory, cognitive and behavioral functions

[5]. Their functional role is currently being investigated both in health and disease [3] under a variety of angles. Of interest here are studies showing that the RSN activity exhibits peculiar scaling properties, resembling dynamics near the critical point of a second order phase transition [6–8]. In addition, there is evidence showing that the brain at rest spends most of the time wandering near a critical point [9]. These empirical findings are consistent with results obtained with computational modeling [10–12].

Here we study whether a simple dynamical model running over the empirical structure of neuroanatomical connections [1] suffices to replicate the aforementioned fundamental features of spontaneous brain activity repeatedly seen in fMRI experiments. The model consists of a network of interconnected nodes (i.e., the connectome), together with a dynamical rule. The matrix of connections follows the neuroanatomical connectivity described recently by Hagmann et al. [1], who studied healthy human subjects and reported the average fiber tract density between any two brain areas (from a gray matter parcellation into 998 areas). To complete the model we need to specify the dynamics of each node. For simplicity, we choose discrete state excitable dynamics following the Greenberg-Hastings model [13]. Thus, each node is assigned a state which can be one of three –quiescent  $Q$ , excited  $E$ , or refractory  $R$  – with the dynamics determined by the transition rules: 1)  $Q \rightarrow E$  with a small probability  $r_1$  ( $\sim 10^{-3}$ ), or if the sum of the connection weights  $w_{ij}$  with the active neighbors ( $j$ ) is higher than a threshold  $T$ , i.e.,  $\sum w_{ij} > T$  and  $Q \rightarrow Q$  otherwise; 2)  $E \rightarrow R$  always; 3)  $R \rightarrow Q$  with a small probability  $r_2$  ( $\sim 10^{-1}$ ) delaying the transition from the  $R$  to the  $Q$  state for some time steps. We held fixed parameters  $r_1$

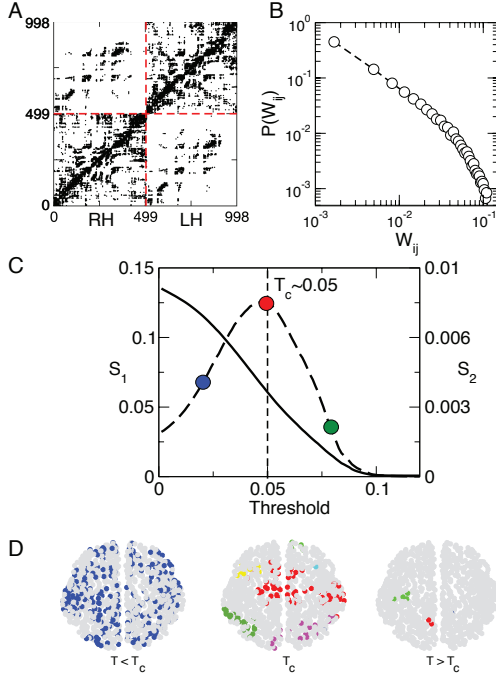


FIG. 1. The model. Panel A shows the model adjacency matrix (i.e., the connectome) and Panel B the edge weights distribution. Data obtained from the white matter tracts connecting a parcellation of 998 nodes covering the entire human brain [1]. RH and LH refers to the right and left brain hemisphere, respectively. Panel C shows the giant cluster's size, (i.e., the order parameter,  $S_1$ , solid line) and the second largest cluster's size ( $S_2$ , dashed line) as a function of the threshold  $T$  (control parameter) as well as the critical point  $T_c \sim 0.05$ . Panel D illustrates examples of clusters (denoted with different colors) at the three  $T$  values denoted with colored markers in Panel C.

and  $r_2$ , which determine the time scales of self-excitation and of recovery from the excited state, respectively, and changed  $T$ . For the numerical analyses, the time series of each node was binarized by assigning state  $E = 1$  and the remaining states into 0's and convolved with a standard hemodynamic response function [14] which mimics the coupling between neural and metabolic activity measured in the fMRI experiments.

As depicted in Figure 1, the dynamics of the model show a transition as a function of the threshold  $T$ . For relatively small values of  $T$  even the weakest connections are enough for the activity to spread, resulting in a regime with a relatively high activity level. On the contrary, for high values of  $T$  the activity only flows through the few strongest connections and therefore the overall activity decreases. To characterize the transition between these regimes an order parameter was defined considering the sizes of the active clusters. Clusters are groups of nodes simultaneously activated and linked to each other through a non zero  $w$ . At each time step the

size of the largest cluster ( $S_1$ ) and the second largest cluster ( $S_2$ ) were computed. These calculations (see Panel C of Fig. 1) unveil a transition between a phase in which a giant cluster covers  $\sim 15\%$  of the system (while the second largest cluster is of negligible size) and another phase in which only scarce activations occur and the nodes fail to coalesce into large clusters. At an intermediate value, a critical point ( $T_c$  in Fig. 1C) can be identified by the peak in the size of the second largest cluster, as done usually in percolation [15] as well as recently in human fMRI experiments [9].

We compare now the dynamics of the model with previous experimental results. In particular, we are interested in two robust features exhibited by the spontaneous activity of human brain RSN [16]: 1) the correlation length of brain activity diverges with size, and 2) the variance of the short-term correlations between pairs of brain sites remains high, independently of the number of pairs considered. Since these two properties are often seen as generic features of criticality, we decided to explore first whether the model exhibits similar dynamics. To be able to compare with the experimental results, we identified each node of the model as belonging to the closest human RSN. This was done by matching the node's coordinates provided by Hagmann et al [1] with a spatial mask of the RSN [4] as done previously [16]. Nodes that were farther than 1 cm away from the closest RSN cluster were discarded from the analysis.

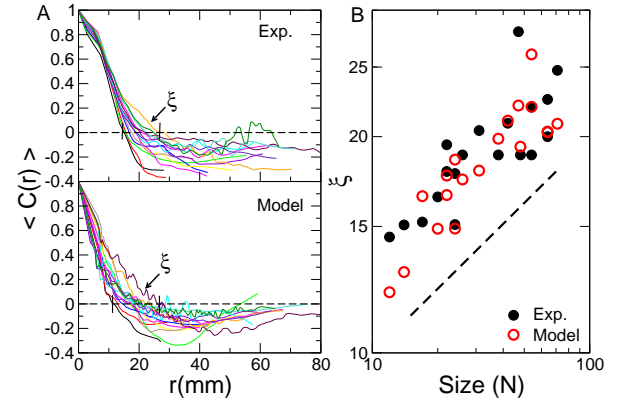


FIG. 2. The correlation length  $\xi$  of the activity in the model near  $T_c$  diverges with the cluster size, as reported for human brain data [16]. Panel A shows the correlation function  $C(r)$  computed from human data (Exp.) and from the model at  $T_c$  (colored lines are used for the different clusters). The correlation length  $\xi$  is the distance  $r$  where  $C(r) = 0$ , seen here to span a range (denoted with the arrows). Panel B shows the  $\xi$  values for the functions plotted on panel A, demonstrating that  $\xi \sim N^{1/3}$  (dashed line), both in the experiment and model data.

*Divergence of the correlation length.* The correlation length represents the average distance at which two points in the system behave independently, and is known

to diverge at criticality [17]. Following a standard procedure [16, 17], we computed the average correlation function of the signal fluctuations between all pairs of nodes in each cluster which are separated by a distance  $r$ , yielding the correlation function  $C(r)$  (details on this computation can be found in the Supp. Info, as well as in [16]).

Fig. 2A corresponds to the two point correlation function as a function of distance for all cluster sizes obtained experimentally and in the model at  $T_c$ . Panel B shows the dependence of  $\xi$  with the cluster size  $N$ . Both numerical estimations clearly show that near  $T_c$  the divergence of the correlation length found in the experiments [16] is reproduced by the model.

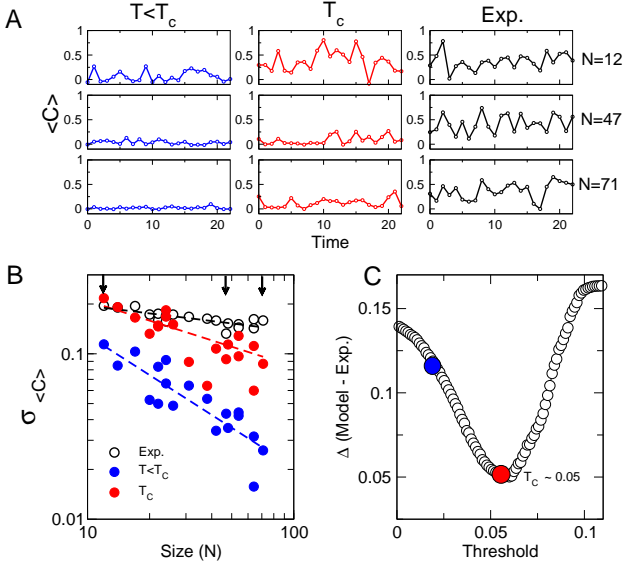


FIG. 3. The short-term correlation  $\langle C \rangle$  in the model at  $T_c$  exhibits transient fluctuations at all cluster sizes as seen in human brain data [16]. Panel A: Examples of  $\langle C \rangle$  fluctuations for three cluster sizes  $N$  at critical ( $T_c$ ) and subcritical ( $T < T_c$ ) dynamical regimes of the model, as well as for the human brain data (Exp.). Panel B shows that the variance of the fluctuations in  $\langle C \rangle$  remains approximately constant only for the human brain data (empty black circles) and for the model at  $T_c$  (filled red circles). For  $T < T_c$  (filled blue circles) the variance decreases faster with  $N$ . The three small arrows denote the sizes used in the examples of Panel A. Panel C shows a plot of the distance between the scaling of the fluctuations of the human fMRI data and those from the model for a wide range of  $T$ . Notice that the best agreement occurs for  $T_c$ . Colored markers in Panel C correspond to the  $T_c$  and  $T < T_c$  values used in Panels A and B.

*Temporal fluctuations of the mean correlation in the RSN.* As recently shown [16], the time evolution of the correlation within these patterns exhibits bursts of high correlation intermixed with instances of dis-coordination. Panel A in Fig. 3 shows examples of the fluctuations in the short-term mean correlation  $\langle C \rangle$  between all pairs of nodes within a given cluster, in this case calculated in non-overlapping time windows of 10 steps. At the critical

state, the variance of  $\langle C \rangle$  is of the same order as observed in the experiments for different cluster sizes. Panel B shows the dependence of the fluctuations in  $\langle C \rangle$  with the cluster size  $N$ . At the subcritical regime the fluctuations decrease as  $\frac{1}{N}$ , which reveals the asynchrony of the active nodes. On the other hand, at the critical state they remain constant, similar to what is observed in experimental fMRI data [16]. In the supercritical regime the vanishingly low level of activity prevents high correlations and therefore the fluctuations amplitude are close to zero for all cluster sizes. To compare with the human fMRI experimental data, we computed the root mean square distance between the model (m) and the experi-

mental data (e) as  $\Delta = \sqrt{\frac{\sum_{N_c} (\sigma_{\langle C \rangle}^{(e)} - \sigma_{\langle C \rangle}^{(m)})^2}{N_c}}$  where the sum is over all clusters  $N_c$ . Panel C shows that the distance is minimum precisely at the critical point of the model.

*RSN spatial patterns emerge only at criticality.* One of the most revealing features of large-scale spontaneous brain activity is its spatial organization into RSN. Their functional relevance is highlighted by the fact that the spontaneous activity closely parallels brain activation patterns seen during task execution [5]. We studied whether these patterns can be seen in the model using the same methods employed to reveal RSN in experimental data (Independent Component Analysis -ICA) as implemented in the FSL MELODIC software [18]. Before proceeding to that, we needed to identify the cortical locations of the model's 998 nodes. For that purpose, the brain gray matter was parcellated via a random growth algorithm (see Supp. Info) using the coordinates of the 998 nodes as seeds. After that, the model time series of each region of interest was assigned to the corresponding parcellation patch (plus Gaussian noise of 0.15 times the variance of the signal), then an ICA decomposition into 8 independent components was performed (a total of 100 trials were performed for each  $T$  value). For each component, we computed the maximal correlation of the model with the spatial location of a set of well-established human RSN [4] obtained with fMRI. As seen in Fig. 4, the correlation  $\langle C_{e-m} \rangle$  peaks near  $T_c$  in all cases. This high correlation implies that the RSN coordinated spontaneous activity unfolds at the same anatomical locations both in the human brain and in the model close to  $T_c$ , something already evident by visual inspection of many of the patterns presented in Fig. 4.

*Discussion.* To the best of our knowledge, this is the first demonstration that a hybrid modeling approach (realistic anatomical connectivity plus a simple dynamical rule) suffices to capture relevant spatio-temporal aspects of dynamics, provided that the dynamical regime is critical. These aspects include generic features of critical systems, but also the emergence of structures having a well-established neurobiological meaning, namely the cortical RSN. While experimental evidence for the afore-

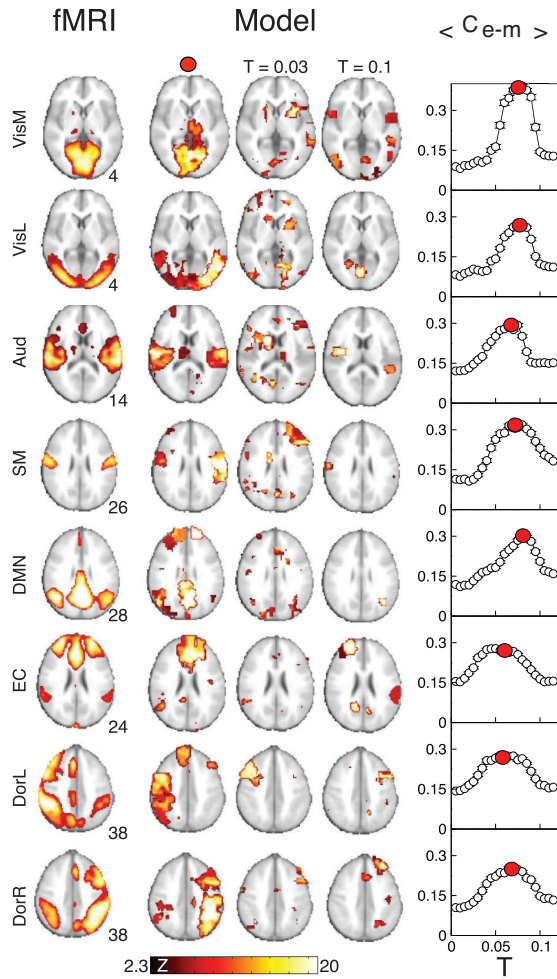


FIG. 4. The spatial organization of the human brain RSN emerges spontaneously in the model near  $T_c$ . RSN obtained from the model with ICA are shown for three values of  $T$ :  $T < T_c$  (0.03),  $T > T_c$  (0.1) and the correlation maxima with the human RSN from [4] (“fMRI”), which is always  $\sim T_c$  (red marker). Right column shows the mean correlation  $\langle C_{e-m} \rangle$  between the spatial location of the experimental human RSN and those obtained from the model as a function of  $T$ . Abbreviations: Medial visual (VisM), lateral visual (VisL), auditory (Aud), sensory-motor (SM), default mode network (DMN), executive control (EC), dorsal visual stream left (DorL) and right (DorR). Numbers beneath each brain slice denote its horizontal coordinate.

mentioned signatures of criticality in brain systems was already discussed [7], in this Letter we made a stronger point: in the model, the critical regime appears as a necessary condition for the emergence of neurobiologically relevant aspects of brain dynamics. Our result also represents an important first step in the direction of realistic hybrid computational modeling of large-scale brain function both in health and disease. As an example, many altered brain states are associated with RSN alterations, a

prominent example being the loss of consciousness in the comatose state [19]. In light of the present results such brain state alterations can be regarded as a displacement from an optimal dynamical point.

Summarizing, the results show that by endowing with critical dynamics the brain network of anatomical connections (or connectome), key observations about brain dynamics can be replicated. These results contribute to close the gap between structural and functional network connectivity in the human brain, by emphasizing the dynamical regime at which models should predict a wide range of observations about large scale brain function.

Supported by CONICET (Argentina), by NIH (USA) and by LOEWE NeFF and BMBF (Germany). We thanks O. Sporns (Indiana University) for sharing the connectome data and C. Beckmann (Imperial College) for the RSN masks reported in [4].

- 
- [1] P. Hagmann, L. Cammoun, X. Gigandet, R. Meuli, C.J. Honey, V.J. Wedeen, O. Sporns, *PLoS Biol.* **6**, e159 (2008).
  - [2] O. Sporns, G. Tononi, R. Kotter, *PLoS Comp. Biol.* **1**, 245 (2005).
  - [3] M.D. Fox and M. Raichle, *Nat. Rev. Neurosc.* **8**, 700 (2007).
  - [4] C.F. Beckmann, M. DeLuca, J.T. Devlin, S.M. Smith, *Philos. T. Roy. Soc. B* **360**, 1001 (2005).
  - [5] S.M. Smith, P.T. Fox, K.L. Miller, D.C. Glahn, P.M. Fox, C.E. Mackay, N. Filippini, K.E. Watkins, R. Toro, A.R. Laird, C.F. Beckmann, *Proc. Natl. Acad. Sci. USA* **106**, 13040 (2009).
  - [6] P. Bak, *How nature works: The science of self-organized criticality* (Copernicus Books, New York, 1996).
  - [7] D.R. Chialvo, *Nature Physics* **6**, 744 (2010).
  - [8] P. Expert, R. Lambiotte, D.R. Chialvo, K. Christensen, H.J. Jensen, D.J. Sharp, F. Turkheimer, *J. R. Soc. Interface* **8**, 472 (2011).
  - [9] E. Tagliazucchi, P. Balenzuela, D. Fraiman, D.R. Chialvo, *Front. Physiol.* **3**, 15 (2012).
  - [10] D. Fraiman, P. Balenzuela, J. Foss, D.R. Chialvo, *Phys. Rev. E* **79**, 061922 (2009).
  - [11] M.G. Kitzbichler, M.L. Smith, S.R. Christensen, E. Bullmore, *PLoS Comp. Biol.* **5**, e1000314 (2009).
  - [12] G. Deco and V. Jirsa, *J. Neurosci.* **32**, 3366 (2012).
  - [13] J.M. Greenberg and S.P. Hastings, *SIAM (Soc. Ind. Appl. Math.) J. Appl. Math.* **34**, 515, (1978).
  - [14] K.J. Friston, C.D. Frith, R. Turner, R.S.J. Frackowiak, *Neuroimage* **2**, 157 (1995).
  - [15] D. Stauffer and A. Aharony, *Introduction to Percolation Theory*, Taylor & Francis, London (1991).
  - [16] D. Fraiman and D.R. Chialvo, *Front. Physiol.* **3**, 307 (2012).
  - [17] A. Cavagna, A. Cimorelli, I. Giardina, G. Parisi, R. Santagati, F. Stefanini, M. Viale, *Proc. Natl. Acad. Sci. USA* **107**, 11865 (2010).
  - [18] C.F. Beckmann and S.M. Smith, *IEEE Trans. Med. Imag.* **23**, 137 (2004).
  - [19] L. Norton, R.M. Hutchison, G.B. Young, D.H. Lee, M.D. Sharpe, S.M. Mirsattari, *Neurology* **78**, 175 (2012).